

Elsevier Editorial(tm) for Sedimentary Geology
Manuscript Draft

Manuscript Number:

Title: Facies, outcrop gamma ray and isotopic signature of exposed Miocene subtropical continental shelf carbonates, North West Cape, Western Australia

Article Type: Research Paper

Keywords: Facies, outcrop gamma ray, C-O isotopes, Miocene, subtropical shelf carbonates, North West Australia

Corresponding Author: Prof. J.F. Read Virginia Polytechnic Institute

Other Authors: Lindsay B. Collins, Ph.D.; James F. Read, Ph.D.; J. W. Hogarth, B.Sc.
Hons; Brian P. Coffey, Ph.D. Curtin University of Technology, Bentley, Western Australia,
Geosciences, Virginia Tech, Blacksburg, Virginia, 24061, U.S.A., Curtin University of
Technology, Bentley, Western Australia , Dept. of Earth Sciences, Simon Fraser
University, Canada

Abstract

ABSTRACT

Exposed Miocene carbonate sequences of the Cape Range, North West Cape, Western Australia, were examined to determine if they preserved a shelf record of paleoclimate, paleoceanographic and eustatic sea level changes during the Miocene. Facies include deep shelf marls (very fine and fine packstone), larger foram wackestone, floatstone and muddy rudstone, foram-coralline algal skeletal fragment packstone-wackestone (shallow seagrass bank facies), lagoonal wackestone/mudstone with scattered corals, gastropods and clams, and tidal flat microbial laminites. Highstand facies of the Early Miocene Mandu-Tulki and Middle Miocene Trealla sequences contain decameter scale (5 to 20 m thick), 4th-order parasequences that shallow and coarsen up, and appear to be due to eccentricity driven sea level changes which may have been up to 50 m. Higher frequency meter-scale parasequences of deep water marl up into larger foram rudstone/floatstone (perhaps obliquity/eccentricity) are evident at the base of the exposed Mandu section. That these are parasequences and not random storm deposits is indicated by the covariance of C and O isotopes, with the heavier values being associated with shallowing and deposition of larger foram facies, and the lighter values associated with deepening and deposition of deep shelf marls.

The uplifted Miocene sediments of the North West Cape thus appear to preserve important sections of continental shelf sediments that can be compared with coeval, better studied deep sea cores. Such studies will enlarge our understanding of the much more poorly studied shelves and their sedimentary record of eustasy, paleoclimate and paleoceanography of the shelves.

INTRODUCTION

The Oligocene to Miocene units of the northwest Australian continental margin form thick prograding units in offshore seismic lines (Figs. 1, 2). Although the gross facies successions have been documented broadly (Apthorpe 1988), the detailed facies makeup of the margin is relatively poorly known. The most recent seismic stratigraphic study of the margin described a relatively small number of ditch cutting samples with respect to grain size and percent carbonate (Young et al. 2001).

The uplifted Cape Range anticline, North West Cape, Western Australia (Fig. 1) provides exposures of these units onshore. Their facies relations, gross lithologies, fossils, and ages have been described by Condon et al. 1955, Chaproniere 1975, Hogarth 1999, and Boterhoven 1999. Outcrop studies in the area are hampered by the weathering of the limestones in this low rainfall setting, which obscures primary fabrics and contacts, necessitating closely spaced sampling or examination of rare core.

In this paper, we measured in detail several outcrop sections, logging bed-by-bed the vertical succession of rock types as identified from fresh samples and in thin section, integrating the data with the petrographic studies of Hogarth (1999) and the foram studies of Chaproniere (1975, 1984). We obtained gamma ray logs of the outcrop sections using a handheld spectral gamma ray scintillometer, in order to evaluate evidence for parasequence- and sequence-scale changes in log signature, and to provide outcrop reference sections for the offshore subsurface. We also have tested whether stable isotopes can be used on the outcrop sections (which potentially preserve a relatively pristine signature, given the arid climate) to evaluate whether high frequency cyclicity in the units is related to random storm influenced processes, or to climatically driven eustatic changes in sea level. Thus, the paper provides a study of Early Miocene highstand facies, the overlying sequence boundary, and the overlying Middle Miocene transgressive and highstand systems tracts.

SETTING

The North West Shelf of Western Australia developed following a single phase (Kaiko and Tait 2001) or two phases of rifting (Veevers and Cotterill 1978, Young et al. 2001), the latest ending by the Middle Jurassic following breakup of Greater India from Western Australia. This was followed by thermo-tectonic subsidence or sag of the passive margin through the later Jurassic and Cenozoic. Cenozoic subsidence rates beneath the shelf have been relatively low (approximately 1 cm/k.y.; Young et al. 2001). High subsidence rates beneath the slope during the Late Eocene to Oligocene were postulated to have a tectonic origin (Apthorpe 1988, Young et al. 2001). However, when water depths estimated from high relief slope clinoforms are incorporated, thermotectonic subsidence becomes negligible on backstripping (Kaiko and Tait 2001). The resulting models show only limited Oligo-Miocene subsidence that is largely due to sediment loading associated with progradation of slope clinoforms into deep water. Uplift of the Cape Range occurred during the Miocene, when parts of the margin were elevated up to 200 to 300 m associated with reactivation of faults deeper in the section (Hocking et al. 1987).

The Oligocene and Miocene continental shelf was a low gradient, distally steepened ramp between 50 and 75 km wide (Young et al. 2001), sloping into water depths of at least several hundred meters, based on foraminiferal faunas and clinoform height (Apthorpe 1988, Kaiko and Tait 2001). In contrast, Young et al. (2001) suggested that the clinoform breakpoint of the progrades lay at depths as shallow as 45 m, and the base of the slope at depths of 150 to 200 m; these depths are underestimated, and are far shallower than their analogous counterparts on the modern shelf (Collins 1988; James et al. 1999) and are not compatible with the foraminiferal data of Apthorpe (1988). Progradation rates of the shelf margin during the Oligocene and Miocene were approximately 1 km/m.y. (Young et al. 2001).

The Oligocene to Middle Miocene succession (Figs. 2, 3) is equivalent to unconformity bounded sequences or cycles 3a and b of Quilty (1977, 1980) and Apthorpe (1988) and to the “Paleogene supersequence” of Young et al. (2001). Onshore, the study interval consists of the Oligocene to Early Miocene Mandu Limestone and Tulki

Limestone and equivalents (sequence 3a), and the overlying Middle Miocene Trealla Limestone (sequence 3b) (Condon et al. 1955, van der Graaff et al. 1980, Quilty 1980, Apthorpe 1988; Fig. 2b).

The Mandu Limestone of sequence 3a unconformably overlies the Late Eocene Giralia Calcarenite and grades updip (east) and to the southwest into a nearshore coarser grained limestone (Bullara Limestone) before pinching out. It thickens to the north and west and is over 300 m thick in the area of Cape Range No. 1 and Shothole Canyon (Fig. 3). The lower Mandu unit (subsurface) is dominated by white to yellow, fine grained marl and fine calcarenite, grading up into an upper outcropping unit of fine limestone with interbeds of larger foram rudstones. The Mandu Limestone is Middle-Late Oligocene to Early Miocene in age, and includes zones P19-21 to N6, whereas the updip Bullara Limestone spans only N3/4 (Fig. 2b; Chaproniere 1984).

The Tulki Limestone (66 to 127 m thick) makes up the uppermost part of sequence 3a and conformably (?) overlies the Mandu Limestone; it is composed of hard, thick bedded white limestone (Fig. 3). At least one minor subaerial disconformity occurs in the transition zone (Chaproniere 1984). The lower Tulki Limestone is a nodular bedded, pinkish-red muddy limestone, overlain by a creamy, massive limestone that is a major cliff former in the Cape Range canyons. The Tulki Limestone is late Early Miocene, and spans N6/7 on the east side of the Cape Range and may be younger (N8) on the west side of the Cape Range (to seaward) (Chaproniere 1984). However, Apthorpe (1988) suggests that it is no younger than zone N6/7 over the Northwest Shelf.

The Trealla Limestone is the updip part of sequence 3b and unconformably overlies the Tulki Limestone (Fig. 3), evidenced by a small gap in the planktonic foram zones (Quilty 1977, Chaproniere 1975) and the presence of synsedimentary collapse features and brecciated and silicified microbial laminites at the base (Hocking et al. 1987). Pisolithic and laminated calcretes noted at the Tulki-Trealla contact (Condon et al. 1955) appear to be a much later Quaternary weathering feature (Hocking et al. 1987). The Trealla Limestone is a hard, white to cream crystalline limestone that has a wide distribution onshore. It is 56 m to over 100 m thick, and consists of a basal microbial laminitite unit, overlain by skeletal packstone with some larger foraminifera similar to the Tulki Limestone but with Marginopora and Astrotrillina, and an upper unit of skeletal

grainstone and milioline forams. In the study area, the Trealla Limestone is no older than N9, and is Middle Miocene (Chaproniere 1984), although Apthorpe (1988) shows it extending from N8 to N11 elsewhere on the North West Shelf. Locally developed quartz sands (Vlaming Sandstone) and sandy and abraded skeletal grainstones (Pilgramunna Formation) are lateral equivalents to the Trealla Limestone along the western Cape Range and may have formed a barrier facies (Chaproniere 1984, Hocking et al. 1987).

METHODS

Gamma ray logs were obtained on measured sections of the upper Mandu Limestone, the Tulki and Trealla limestones using a handheld Exploranium^R spectral gamma ray scintillometer, with readings taken at 1 m intervals, with the instrument calibrated at the start of each day. Counts for K, U and Th were recorded along with total counts. Stable isotopes were sampled every 33 cm (3 per meter) from a section at the base of the exposed section of Mandu Limestone at Shothole Canyon, from which a gamma ray log had been obtained. The section selected was composed of interbedded marl and larger foram limestones. Isotopes were not collected from higher units because of the reported subaerial modification believed to have affected these. In the laboratory, a portion of the mud matrix of the marl and foram rudstone (which are mud dominated, spar-poor sediments) was sampled using a dental drill mounted in a bench milling machine, with care being taken to avoid sampling the larger skeletal components in order to avoid the effects of biological fractionation. C and O isotope values were analyzed by Dave Winter at H. Spero's laboratory, University of California, Davis.

FACIES

A schematic depositional profile of the facies is shown in Figure 4 and facies are summarized in Table 1, based on data in Chaproniere (1975, 1984), Hogarth (1999) and this study. Detailed stratigraphic columns of units are shown in Figures 5 to 7. Cross plots of gamma ray data are shown in Figure 8, and a cross plot of the isotopic data is shown in Fig. 9.

Facies (Table 1, Fig. 3) are listed below from deep to shallow. Estimates of water depths of depositional facies are based on foraminiferal paleoecology by Chaproniere (1975, 1984).

Very fine to fine grained wackestone-packstone (marl): These fine grained wackestone-packstone or marl (Table 1) in the lower Mandu in the subsurface formed in outer continental shelf, largely subphotic depths perhaps greater than 120 m, based on percent planktics, lack of calcareous algae or larger forams. The exposed upper Mandu fine packstones or marls formed in slightly shallower photic depths (60 m to less than 100 m) based on their lower planktic values, and presence of some algae and larger benthics (*Operculina complanata* and *Cycloclypeus eidae*). Very fine to fine packstones also occur in the Tulki Limestone parasequences, although their low planktic percents (0 to 3) suggest shallow depths of a few tens of meters (Chaproniere 1975).

Larger-foram packstone, floatstone, rudstone: These larger-foram beds (Table 1) occur in the base of the exposed, upper Mandu section (Figs. 4 and 5). They contain *Lepidocyclina badjirraensis-Cycloclypeus eidae*, and probably formed in depths from 15 m to less than 60 m, based on the low planktic percent, and the presence of large and small forams that have symbionts today. These formed below the depths of abundant grasses, although the larger forams may have formed a baffle (Chaproniere 1975). The upper units of larger foram packstone-grainstone in the Mandu contain *Lepidocyclina howchini-Cycloclypeus eidae* and some evidence of seagrass encrusters suggesting depths less than 12 m according to Chaproniere (1975).

Skeletal Wackestone: Skeletal wackestones with a fine skeletal peloid matrix are common in the Tulki and the Trealla Limestones (Table 1). In the Tulki Limestone, these have relatively open marine shallow foram assemblages with some larger forams (*L. howchini* and *Cycloclypeus*), rare to no planktic forams, and biotas that suggest possible seagrass cover locally. Wackestones in the upper Trealla have the *Astrotrillina-Flosculinella* assemblage with abundant miliolines, *Marginopora*, *Peneroplis*, encrusting- and attached forams, alveolinids, stick corals and coralline algae that support shallow water depths and sea grass cover, with metahaline salinities (Chaproniere 1975); these developed behind the quartzose barrier system (Pulgramunna Formation) that caused restriction to the east.

Skeletal fragment packstone and grainstone: These skeletal fragment grainstone-packstones (Table 1) in the lower Tulki have the *Lepidocyclus howchini*-*Cycloclypeus* assemblage similar to the upper Mandu beds, but also contain numerous seagrass encrusters (coralline algae and encrusting forams) suggesting relatively shallow water depths. Upper Tulki and basal Trealla grainstone-packstone contains the *L. howchini*-*Marginopora vertebralis* association and low planktic percentages, suggesting seagrass baffles, relatively shallow depths less than 20 m and possible metahaline condition (Chaproniere 1975).

Restricted Lime Wackestone/Mudstone: These relatively poorly fossiliferous facies in the uppermost Tulki and the basal Trealla (Table 1) are restricted low energy lagoon or embayment facies that formed nearshore, locally under elevated salinities. Restriction may have been due to development of a barrier system along the western (oceanic) side of the present Cape Range, which in the Trealla equivalents is manifested by the Pilgramunna cross-bedded quartz-skeletal grainstones (Chaproniere 1975).

Microbial Laminites: These occur in dolomitized thin beds in the basal Trealla Limestone (Table 1). They are tidal flat facies that formed perhaps under semi-arid conditions, judging by the scarcity of burrowing in the laminites, although conditions were never sufficiently restricted to form evaporates. Brecciation and slumping of these facies appears to have developed during emergence.

SEQUENCES AND PARASEQUENCES

Sequence 3a: Mandu-Tulki Limestone

The Mandu-Tulki interval logged here forms the highstand systems tract of a major depositional sequence bounded at the base and top by unconformities in the study area (Fig. 3). The logged section of Mandu Limestone overlies a thick (over 200 m) subsurface section of deep water, friable, marly fine grained packstone, with small benthic and abundant planktic forams, along with larger benthic forams that increase up-section (*Operculina*, *Lepidocyclus* and *Cycloclypeus*; Chaproniere 1984). The exposed upper Mandu section logged is an 80 m thick, coarsening upward succession and consists of deeper water marl and thin beds of larger foram packstones that become thicker upward (Fig. 5). The conformably overlying Tulki Limestone at Shothole Canyon is over

60 m thick and forms an overall upward fining succession. The lower Tulki Limestone consists of larger foram-skeletal wackestone to skeletal fragment packstone/grainstone units. The upper Tulki is upward fining, dominated by wackestone and lime mudstone, capped by brecciated, silicified microbial laminites (Fig. 5).

Decameter-scale Parasequences: The exposed Mandu-Tulki coarsening-upward succession (Fig. 5) consists of several decameter-scale coarsening upward parasequences. The parasequences in the exposed Mandu Limestone are 5 to 20 m thick, and they tend to become thinner up section into the lower Tulki Limestone. The Mandu parasequences consist of deeper water, planktic foram-bearing very fine to fine skeletal packstone (marl) with thin larger-foram interbeds, shallowing up into caps of larger-foram packstone/floatstone/rudstone (Fig. 5; Table 1). The marl intervals become slightly coarser (fine to medium grained) and grainier upward in the Mandu Limestone as part of the overall upward coarsening trend.

There are up to five parasequences in the overlying lower Tulki Limestone (Fig. 5). They are 5 to 10 m thick and consist of nodular, very fine to medium grained, skeletal fragment packstone-wackestone (with scattered large forams) and rarely mudstone, capped by larger foram packstone/rudstone, or higher in the section, by shallow water, coarse to very coarse, skeletal fragment grainstone/packstone with seagrass skeletal assemblages; parasequence caps change from oceanic biotas to metahaline biotas upsection (Fig. 3, Table 1; Chaproniere 1975). Parasequences are difficult to recognize in the upper ten meters of the Tulki Limestone, which consists of fine grained peloid skeletal packstone, wackestone and lime mudstone containing scattered silicified corals; it is capped by brecciated microbial laminate of the basal Trealla Limestone (Fig. 5).

Overall the Mandu-Tulki interval has a sawtooth gamma ray pattern, characterized by an overall upward-decreasing gamma ray signature from the Mandu up into the lower Tulki Limestones, and then a relatively uniform but jagged response in the upper Tulki Limestone (Fig. 5). Highest values occur in the fine grained, siliceous marls in the lower part. The decameter-scale parasequences have a gamma ray signal characterized by a broadly upward decreasing signal into the more grainy facies; bases of some parasequences show a thin zone of upward increasing response before decreasing

upward (Fig. 5). There is a distinctive superimposed jagged, sawtooth pattern with a 1 to 2 m wavelength superimposed on these larger scale trends.

High Frequency Parasequences – Mandu Limestone: Meter-scale high frequency parasequences of marl up into larger-foram rudstone-floatstone occur in the basal portion of the exposed Mandu Limestone (Fig. 6). Many of the coarser grained, larger foram beds capping the meter-scale parasequences have relatively sharp basal contacts, some of which show large burrows extending down into the underlying marl unit. Matrix in the coarser beds is similar to the marl and is very fine- and fine-packstone and in a few coarse beds the larger forams have fanned arrangements. The isotopic and lithologic data suggest that some of the parasequences are bundled into larger parasequences about 4 to 5 m thick (Fig. 6).

At the scale of the meter-parasequences, there is little correlation between the gamma ray signal and the facies, except that the highest gamma ray values locally coincide with the thicker marls. The gamma ray signature of some parasequence sets appears to show low gamma ray values in the grainy facies, and high gamma ray values in the marl facies (Fig. 6). There is little correlation between the stable isotope values and the gamma ray counts.

The C and O isotope values for the sampled Mandu Limestone strongly covary, with high carbon isotope values corresponding to high oxygen isotope values (Figs. 6, 9). In general, the most negative values occur in the finer grained, deeper water facies, while the more positive values occur in the muddy, coarser grained units with abundant larger benthic forams (Fig. 6). Individual parasequences may show decreasing carbon and oxygen values above the flooding surface, reaching a maximum in the marl, and then decreasing upward into the larger-foram units. Oxygen isotope values (PDB) range from -2 to -3 per mil for the more negative values, to -1 to +1 per mil for the more positive values; thus most of the shorter term excursions have a range of 2 per mil or less, with one excursion with a range of 4 per mil. Longer-term trends show that the oxygen isotope values become more negative into the more mud-dominated deeper water intervals, and more positive in the more grainy shallow water dominated intervals; this is compatible with the high frequency trends.

The covarying C isotope values (PDB) show similar trends to oxygen, but show much narrower ranges. The more positive values are around +1 per mil while the more negative excursions range down to zero.

Sequence 3b: Trealla Limestone

The unconformity bounded Trealla Limestone (Figs. 3, 7) is a 40 m thick depositional sequence in the studied sections. The basal Trealla consists of at least two silicified and dolomitic microbial laminites interlayered with fine grained wackestone-mudstone and dolomite (Figs. 3, 7; Table 1). The laminites are locally brecciated and disrupted, and thus mark the sequence boundary; the reported calcretes associated with the Tulk-Trealla contact are a much younger overprint (Hocking et al. 1987). The Trealla Limestone coarsens up into open marine, skeletal grainstones and packstones (with echinoderms, larger and smaller benthic forams, red algae, peloids). These then fine up into wackestones and mudstones, with local silicified coral heads and sticks, forams (soritids, miliolids, rare larger forams) and echinoderms (Figs. 3, 7; Table 1).

Decameter-Scale Parasequences: At least three parasequences occur in the Trealla section logged (Fig. 7). At Shothole Canyon, the basal Trealla parasequence is a carbonate mudstone to microbial laminites. This is overlain by the deepening upward part of a partial parasequence (dolomitized coral- and gastropod-wackestone-mudstone to fine packstone with scattered bryozoans; Fig. 7).

The overlying parasequences occur in the slightly younger Trealla section at Swan Cement quarry (Fig. 7). The lowest cycle here is upward coarsening with pelagic foram-larger foram skeletal fragment wackestones shallowing up into lithoclastic-larger foram skeletal fragment packstone-grainstone (*L. howchini-Marginopora* seagrass assemblage) (Fig. 3; Table 1). This is overlain by a parasequence consisting of deepening upward, larger foram-coralline packstone and algal bindstone to large foram wackestone (locally dolomitized), shallowing up into skeletal fragment packstone (*L. howchini-Marginopora* assemblage). The top of the section consists of over 8 m of skeletal wackestone with the *Astrotrillina-Flosculinella* assemblage (metahaline

seagrass associated facies) that lacks the open-marine larger forams (Chaproniere 1975; Table 1). It is not clear whether these wackestones belong to a new parasequence related to slight deepening, or whether the change from the underlying packstone up into wackestone is due to increased abundance of sea grass baffles. The upper contact of the Trealla has been erosionally truncated by post-Miocene erosion in the studied section.

The Trealla Limestone has an overall upward decreasing then upward increasing gamma ray response (Fig. 7). There is a jagged sawtooth pattern superimposed on this. High gamma ray values are associated with peritidal laminated intervals at the base of the Trealla and with intraclastic peloid foram units in the lower part of the Trealla (Fig. 7). The gamma ray response decreases toward the top of the upward coarsening portion in the middle of the Trealla Limestone. It then increases into the muddy wackestones in the upper part of the Trealla section (Fig. 7).

INTERPRETATION

Large Scale Parasequence Development: Late Oligocene sea level fluctuations of up to 50 m or so occurred in the Late Oligocene (Kominz and Pekar 2001). These are accompanied by $\delta^{18}\text{O}$ shifts averaging about 0.7 per mil in the $\delta^{18}\text{O}$ record of the deep sea (Zachos et al. 1997) excluding the large oscillation at the Oligocene-Miocene boundary. Oxygen isotope excursions right at the Oligo-Miocene transition suggest large cooling and ice buildup events and associated sea level excursions (Zachos et al. 1997). However, the Early Miocene $\delta^{18}\text{O}$ curves from above the Oligo-Miocene boundary in the deep sea (Zachos et al. 1997, Billups et al. 2002) are similar in magnitude to those of the Late Oligocene, suggesting that apart from the boundary, Late Oligocene and Early Miocene sea level fluctuations might have been similar, and about 50 meters or so, all other conditions being equal. A strong 400 k.y. cyclicity, along with an obliquity and perhaps precessional signal is evident in the deep sea record (Zachos et al. 1997, Billups et al. 2002, Williams et al. 2002).

Calculated accumulation rates in the study area during the Oligo-Miocene were 3 to 4 cm/k.y. These reflect, in part, unfilled accommodation on the ramp and are higher than subsidence rates. This would suggest that 400 k.y. cycles likely would be in the range of 12 to 16 m thick, compatible with the decameter scale cycles being related to

long-term eccentricity while the meter scale cycles may be 5th-order cycles (20 to 40 k.y.).

Given the outer shelf depths of the Mandu marls in lower parts of large scale Mandu parasequences, upward shallowing during deposition of even a 20 m thick parasequence would not have caused the resulting upward facies change. Rather, they would need additional superimposed sea level rise and fall of perhaps tens of meters related to long-term eccentricity.

Similarly in the lower Tulki Limestone, parasequences composed of fine nodular limestones deposited in water depths of some tens of meters, overlain by relatively coarse skeletal packstone and grainstone deposited in less than 15 m, require eustatic sea level changes because upward shallowing by sedimentation would be insufficient to provide the change in water depths required. The upper Tulki Limestone, which has a single 20 m thick parasequence composed of relatively shallow inner shelf facies, capped by tidal flat laminites, is perhaps related to filling of a lagoon behind a barrier which may have led to metahaline salinities.

Trealla parasequences in the study area reflect progressive submergence of a previously emergent platform under oscillating sea levels. This resulted in a thin peritidal parasequence at the base, overlain by two relatively open marine parasequences, with maximum water depths of 20 m and metahaline salinities during formation (Chaproniere 1975). These slightly elevated salinities probably are due to the Trealla carbonates having formed landward (east of) the barrier system of sandy grainstone (Pilgramunna Formation) along the western region of the present Cape Range (Chaproniere 1975).

Water depths for much of the Mandu-Tukli-Trealla succession appear to have been too great for significant exposure of the shelf in the study area, if 50 m sea level changes were involved. However, as the shelf shallowed, these sea level changes probably would have affected shallow parts of shelves under 50 m causing wave sweeping and photic conditions in previously deeply submerged areas. However, subaerial surfaces capping parasequences are rare (Chaproniere 1975). Whether such exposure surfaces are indeed absent, or their nonrecognition was due to the modern tufa cover masking any exposure surfaces, is not clear. Given the low rates of subsidence of the platform, shallow water parasequences in the Tulki and the Trealla Limestones likely

would have been exposed during sea level fall, unless sea level fluctuations decreased in magnitude during deposition of the upper Mandu to Trealla succession.

Interpretation of Gamma Ray Response: The relatively high total gamma ray response of the deeper water facies is associated with marine flooding events within many of the Mandu Tulki decameter scale parasequences. This is likely due to higher radioactive K contents associated with increased phyllosilicate clay and fine felspar concentrations and in the deeper finer grained facies (Rider 1996). The weaker correlation between total gamma ray counts and U perhaps is related to some addition of Uranium bound up in organics in the deeper water facies. Thorium, being generally associated with fine siliciclastics and heavy minerals (Rider 1996), does not show much correlation with total gamma ray response. The shallower, coarser grained facies have progressively decreasing gamma ray counts due to winnowing of fines with shallowing, perhaps along with slightly decreased organic matter concentrations. The role of wet-dry cycles in the hinterland in controlling the K-bearing clay contents in the sediments is not clear, but if a factor, would relate to increased runoff during higher sea level and warmer phases, and decreased runoff during colder lowered sea levels. The parasequences higher in the Mandu-Tulki and the lower and upper Trealla succession formed in shallower settings. The increased gamma counts of the shallower water facies, perhaps could be associated with detrital clays and felspars being shed out onto the much shallowed platform during sea level falls.

Interpretation of Stable Isotope Signal, and High Frequency Mandu Cycles: The association of heavier $\delta^{18}\text{O}$ values with the shallower water foram units suggests that the oxygen isotopes are recording lowered sea levels, likely related to increased ice volume at the poles, possibly coupled with cooler temperatures of calcite precipitation. Conversely, the light values associated with the deepening events, would appear to relate to decreased ice volume, melting, and local, warmer bottom temperatures. It is not possible to separate out the effects of cooling versus ice volume given the present data set. The range is far larger than that from Late Oligocene and Early Miocene deep sea cores in which the fluctuations are less than 1 per mil (Zachos et al. 1997). Given that the

Pleistocene oxygen isotopes from the deep sea cores show roughly 1 per mil per 100 m of sea level change where the signal is largely related to ice volume (Hays et al. 1976), it is unlikely that the deep shelf Mandu $\delta^{18}\text{O}$ values are solely due to ice volume, given their relatively large ranges. They are not the result of diagenetic resetting, because during shallowing (and possible emergence) they should be reset to lighter oxygen (and carbon) values, which is not evident; rather the heavier values are associated with the shallower facies, suggesting global ice buildup and sea level fall, coupled with cooling of the shelf waters. Thus, they also reflect significant cooling of bottom shelf waters during sea level fall, and warming of shelf waters during later stages of sea level rise. This might have been accompanied with increased salinity and evaporation of the shelf waters during sea level lowstands which would further increase the $\delta^{18}\text{O}$ values.

A second implication is that the interbedding of the coarse foram units with the finer marl units in the high frequency Mandu cycles is not merely the result of storm processes bringing coarse material out onto the shelf (as proposed for many such successions elsewhere; Aigner 1982, Racey 2001). Instead they appear to be due to eustatic and climatic sea level changes that caused periodic shallowing (increasing the effects of storm processes on the bottom) followed by deepening of the shelf. With shallowing, benthic foram facies were deposited on the shelf, and the lowered wave base allowed storm reworking of these deposits. As sea level rose, these facies were succeeded by fine carbonates deposited largely below wave base. With renewed shallowing, the upper surfaces of these facies were burrowed, the burrows becoming filled with coarse foram debris.

The covariance of the oxygen and carbon isotopes (Figs. 6, 9) is strikingly similar to that from the deep sea western Atlantic described by Zachos et al. (1997). Burial of organic carbon influencing global marine C reservoirs tends to occur at longer time scales (Holser 1997). Short-term positive carbon isotope excursions relate to increased productivity in surface waters and preferential extraction of light carbon from the shallow water mass by planktic organisms, as in the modern oceans (Holser 1997). In addition, sea level falls would have brought the carbonate factory into contact with waters isotopically heavier in C. The covariance of carbon and oxygen has been explained by increased surface productivity during the cooler glacial stages due to increased

circulation (Zachos et al. 1997). The lighter values of the deeper water facies may be due to decreased extraction of light carbon in the deeper waters, leaving them relatively unmodified, and retaining their relatively light C signatures.

The lack of covariance between the gamma ray counts and oxygen/carbon isotopes in the Mandu high frequency cycles in part results from the fact that the gamma ray peaks (which are relatively small, below 40 counts) only correlate with the deeper water facies in 50% of cases. The gamma ray variation at this scale may be noise. Note also that fines are common in most of the facies and so the coarser grained beds are not winnowed free of fines and clays. However, the approximately 5 to 10 m thick bundles of high frequency cycles form shallowing up parasequence sets which tend to show an upward decreasing (albeit jagged) gamma ray response, characteristic of the decameter scale parasequences higher in the Mandu-Tulki units.

Significance: This study illustrates that gamma ray logs collected using a handheld scintillometer, through the onshore Miocene carbonates of northwestern Australia, can be used to define broad, sequence scale, upward-deepening and upward-shallowing trends (Young et al. 2001). Perhaps more importantly at a smaller scale, they also can be used to define parasequences. In conjunction with lithologic logs and perhaps well cuttings, they potentially could be used to generate a high resolution sequence stratigraphy for the Oligo-Miocene succession of the region. However, this integration of the lithology and gamma ray log is essential, because the high gamma ray values occur both in the deeper facies, as well as the shallowest facies.

The study also suggests that the deeper shelf Miocene Mandu Limestone preserves a relatively pristine carbon and oxygen isotope signature. This raises the possibility that the deeper shelf, onshore Oligo-Miocene could be cored in order to obtain a longer-term record of oceanographic changes that affected the shelf during deposition, during this time of important global climate change. This record could shed light on the combined effect of global ice volume and temperature, as well as high frequency productivity changes on the shelf. Because much of the global climate data is from the deep sea, recovery of deep shelf sections with paleoclimate information could provide

much insight into global and local climatic, oceanographic and productivity cycles within the context of continental shelves rather than ocean basins.

CONCLUSIONS

Handheld gamma ray readings and isotopic analyses were obtained for outcropping Miocene subtropical carbonates at Shothole Canyon in the Cape Range, North West Cape, Western Australia. The units sampled were the Early Miocene highstand portion of the Mandu-Tulki Limestones and the transgressive and highstand part of the Middle Miocene Trealla Limestone. Facies include deep shelf marls (very fine and fine packstone), larger foram wackestone, floatstone and muddy rudstone, foram-coralline algal skeletal fragment packstone-wackestone (shallow seagrass bank facies), lagoonal wackestone/mudstone with scattered corals, gastropods and clams, and tidal flat microbial laminites. The handheld gamma ray records clearly show the large scale sequence stratigraphic units, with an overall decreasing or "cleaning-upward" gamma ray response in the Mandu-Tulki highstand carbonates, and an increase in the gamma ray response near the upper sequence boundary on the Tulki Limestone. Several 4th-order "cleaning upward" decameter scale parasequences (5 to 20 m thick) are evident in the highstand. These likely are due to significant 4th order sea level changes, evident in contemporaneous published deep sea isotope records. The transgressive to highstand Trealla Limestone shows a similar upward-decreasing then upward increasing gamma ray response.

The lower exposed portion of the Mandu Limestone is dominated by meter scale, marl-larger foram rudstone units. The meter scale units are not evident on the gamma ray logs, which appear to be responding to larger (decameter) scale bundles, in which the dominantly deeper water facies show high gamma ray response and the shallower water units show a lower gamma ray response. C and oxygen isotopes covary, with the deeper water marls being light, and the shallower water larger foram packstones being isotopically heavy. This is opposite to what one would expect of a diagenetic signal related to syndepositional emergence, for which there is little physical evidence. The light oxygen values of marls may reflect decreased global ice volume and higher

temperature bottom waters relative to the larger foram packstones. The carbon isotope signal shows lightest values in the deep water facies. This may reflect sea level fluctuations with the deep water facies sampling isotopically light carbon in the deep shelf waters, while the shallower water carbonates sampled C enriched shallow shelf waters, reflecting high productivity. The C signature could also reflect increased productivity cycles on the deep shelf during glacially driven high frequency lowstands, and decreased productivity during high sea levels. The isotopic data indicates that the marl-larger foram cycles are not randomly interbedded storm deposits, but likely are 5th-order parasequences formed by significant high frequency changes in sea level on the deep shelf.

ACKNOWLEDGMENTS

Fred Read would like to thank Lindsay Collins and Curtin University for support during tenure of a John Curtin International Fellowship and for hospitality during several visits to Western Australia, and to Virginia Tech for six months of leave on Research Assignment. Isotope analyses were done by Howie Spero's Stable Isotope Laboratory, University of California, Davis, courtesy of Dave Winter. We would like to thank Thomas Wynn for help with the handheld gamma ray scintillometer data gathering and analysis, and Ellen Mathena for editing and word processing.

REFERENCES

- Aigner, T.** (1982) Event stratification in nummulitic accumulations and in shell beds from the Eocene of Egypt. In: *Cyclic and Event Stratification*, (Eds G. Einsele and A. Seilacher), pp. 248-262. Springer-Verlag.
- Apthorpe, M.** (1988) Cainozoic depositional history of the North West Shelf. In: *The North West Shelf, Proceedings of the North West Shelf Symposium* (Eds P.G. and R. R. Purcell), pp. 55-84. Perth, Western Australia.

Billups, K., Channell, J. E. T. and Zachos, J. (2002) Late Oligocene to early Miocene geochronology and paleoceanography from the subantarctic South Atlantic. *Paleoceanography*, **17**, 4-1 to 4-11.

Boterhoven, B. (1999) Lithofacies and depositional environments of the Cardabia and Giralia Calcarenites, Giralia Anticline, and subsurface correlatives of the Exmouth Sub-basin, Western Australia, Honours Thesis (Applied Geology), Curtin University, Perth, Western Australia, 99 p.

Chaproniere, G. C. H. (1975) Paleoecology of Oligo-Miocene larger Foraminiferida, Australia. *Alcheringa*, **1**, 37-58.

Chaproniere, G. C. H. (1984) Oligocene and Miocene larger Foraminiferida from Australia and New Zealand. *Department of Resources and Energy, Bureau of Mineral Resources, Geology and Geophysics, Bull. 188*, Australian Government Publishing Service, Canberra, 98 p., 26 plates.

Collins, L. B. (1988) Sediments and history of the Rottnest Shelf, southwest Australia: a swell-dominated, non-tropical carbonate margin. *Sedimentary Geology*, **60**, 15-49.

Condon, M. A., Johnstone, D., Perry, W. J. and Crespin, I. (1955) The Cape Range structure, Western Australia. *Bulletin Bureau Mineral Resources, Geology and Geophysics, Australia*, **21**, 1-82.

Davies, G. R. (1970) Carbonate bank sedimentation, Eastern Shark Bay, Western Australia. *Memoir American Association of Petroleum Geologists*, **13**, 85-168.

Hays, J. D., Imbrie, J. and Shackleton, N. J. (1976) Variations in the Earths orbit: pacemaker of the ice ages. *Science*, **194**, 1121-1131.

Hocking, R. M., Moors, H. T. and van de Graaff, J. E. (1987) Geology of the Carnarvon Basin, Western Australia. *Geological Survey of Western Australia, Bull. 133*, Perth, Western Australia, 89 p.

Hogarth, J. W. (1999) Lithofacies and depositional environments of part of the Cape Range Group, Exmouth Sub-Basin, Western Australia. Honours Thesis (Applied Geology), Curtin University of Technology, Perth, Western Australia, 92 p.

Holser, W. T. (1997) Geochemical events documented in inorganic carbon isotopes. *Paleoceanography, Paleoceanography, Paleoclimatology, Paleoecology*, **132**, 173-182.

James, N. P., Collins, L. B., Bone, Y. and Hallock, P. (1999) Subtropical carbonates in a temperate realm: modern sediments on the southwest Australian shelf. *Journal of Sedimentary Research*, **69**, 1297-1321.

Kaiko, A. R. and Tait, A. M. (2001) Post-rift tectonic subsidence and paleo-water depths in the northern Carnarvon Basin, Western Australia. *APPEA Journal*, 367-379.

Kominz, M. A. and Pekar, S. F. (2001) Oligocene eustasy from two-dimensional sequence stratigraphic backstripping. *Geological Society of America Bulletin*, **113**, 291-304.

Quilty, P. G. (1977) Cenozoic sedimentation cycles in Western Australia. *Geology*, **5**, 336-340.

Quilty, P. G. (1980) Sedimentation cycles in the Cretaceous and Cenozoic of Western Australia. *Tectonophysics*, **63**, 349-356.

Racey, A. (2001) A review of Eocene nummulite accumulations: structure, formation and reservoir potential. *Journal of Petroleum Geology*, **24**, 79-100.

Rider, M. H. (1996) *The Geological Interpretation of Well Logs*. Blackie, Halsted Press, John Wiley and Sons, 280 p.

Van der Graaff, W. J. E., Denman, P. D., Hocking, R. M. and Baxter, J. L. (1980) Explanatory Notes on the Yanrey-Ningaloo 1:250,000 Geological Series, Geological Survey of Western Australia, Perth, Western Australia, 1-24.

Veevers, J. J. and Cotterill, D. (1978) Western margin of Australia: evolution of a rifted arch system. *Geological Society of America Bulletin*, **89**, 337-355.

Williams, T., Kroon, D. and Spezzaferri, S. (2002) Middle and Upper Miocene cyclostratigraphy of downhole logs and short- to long-term astronomical cycles in carbonate production of the Great Bahama Bank. *Marine Geology*, **185**, 75-93.

Young, H. C., Lemon, N. M. and Hull, J. N. F. (2001) The Middle Cretaceous to Recent sequence stratigraphic evolution of the Exmouth-Barrow margin, Western Australia. *APPEA Journal*, **41**, 381-413.

Zachos, J. C., Flower, B. P. and Paul, H. (1997) Orbitally paced climate oscillations across the Oligocene/Miocene boundary. *Nature*, August 1997, 567-570.

FIGURE CAPTIONS

Fig. 1. Locality map showing location of North West Cape and sections measured in this study. Regional setting shown on inset map.

Fig. 2. Regional cross section redrawn from seismic reflection profile (Line C of Young et al. 2001) showing regional distribution of Oligo-Miocene units. Section location and relation to North West Cape is shown on inset map (based on data in Young et al. 2001).

Fig. 3. Generalized cross section showing stratigraphic relationships in the North West Cape area, modified from Chaproniere (1984). Dotted lines show inferred regional clinoforms based on the biostratigraphy (planktic foram zones are labeled N2 to N9 and P19/20). Brick pattern - shelf carbonates; gray shading - deeper shelf and slope carbonates.

Fig. 4. Schematic depositional facies profile of the Oligo-Miocene units, North West Cape. A barrier (not shown) likely existed between the study area and the open shelf along the western margin of the Cape Range during Upper Tulki and Trealla deposition.

Fig. 5. Measured section of Miocene Shothole Canyon section spanning Mandu and Tulki Limestone, showing lithologic succession and outcrop gamma ray response. Section shows distinct 4th-order upward shallowing parasequences evident on both the lithology log and the gamma ray log.

Fig. 6. Detailed measured section of cyclic units in base part of Mandu section, Shothole Canyon. Gamma ray profile shows several large scale cycles, but the C-O isotopic data covary, with light values associated with the deeper water facies and heavy values associated with shallow water facies.

Fig. 7. Measured section of Trealla Limestone, Swan Cement Quarry, showing lithologic succession and outcrop gamma ray response.

Fig. 8. A. Cross plot of total K counts versus total gamma ray counts, Mandu-Tulki section, Shothole Canyon, showing that the signal likely reflects K in clays in the carbonates. B. Cross plot of U counts versus total gamma ray counts, showing that U has contributed only a moderately to the total gamma ray response. C. Cross plot of Th to total gamma ray counts, showing that Th contributes little to the total gamma ray response.

Fig. 9. Cross plot of carbon and oxygen stable isotopes, showing their strong positive covariance.

Table

Facies	Very fine to fine packstone (“marl”)	Larger foram packstone, floatstone, rudstone	Skeletal wackestone	Skeletal fragment packstone and grainstone	Restricted skeletal fragment wackestone and lime wackestone/mudstone	Microbial laminite
Environment	Deeper oceanic waters, below wave base. Upper Mandu: >60m. Lower Mandu: planktic foram-rich units >120m	Above storm wave base, 15m to 60m depths. Oceanic salinities	Shallow water, moderate to low energy, possible seagrass influence. Oceanic to possibly metahaline	Shallow water depths less than 15m; possible seagrass covered substrates. Oceanic to possibly metahaline	Restricted low energy embayment and lagoon. Metahaline to hypersaline	Tidal flat, hypersaline
Occurrence	Mandu	Mainly Mandu and lower Tulki	Upper Mandu, Tulki and lower Trealla limestone	Mainly in Tulki and lower Trealla	Uppermost Tulki and basal and upper Trealla	Basal Trealla limestone
Color	White to pale yellow	Cream-colored	White to cream	White to pale yellow	Gray	Tan weathering, gray
Bedding/ Sedimentary Structures	Massive, burrowed to poorly laminated	Thin beds in marl, layered, commonly flat-lying tests, some imbricate fans	Massive to poorly bedded.	Thick bedded to massive units	Massive to layered	Wavy and crenulated microbial lamination and fenestral voids; brecciated and contorted locally
Sediment Description	Very fine to fine packstone of abundant planktic forams, scattered larger benthic forams, fine skeletal debris (including much fine echinoderm and some bryozoa), 5 to 25% quartz silt and some clay	Gravel-sized packstone, floatstone and rudstone of abundant larger forams, in matrix of fine peloids and skeletal debris including planktic forams, bryozoans, echinoids, and in upper units coralline algae. Some quartz silt and clay.	Skeletal wackestone with planktic forams rare to absent; composed of fine skeletal debris, peloids and lime mud, with larger skeletal debris (larger forams and small benthic forams, coralline algae, echinoderm) floating in fine peloidal-skeletal packstone or mud matrix. May be recrystallized to microspar and spar in Upper Tulki	Poorly sorted, sand and gravel-sized packstone-grainstone of fragmented skeletal debris (echinoderm, larger forams, smaller benthic forams, coralline algae) in a very fine and fine peloid packstone and mud matrix. Range from mud lean to mud rich	Range from skeletal wackestone (skeletal fragments, miliolids, <i>Marginopora</i> , alveolinids, <i>Flosculinella</i> , encrusting forams, coralline algae) to poorly fossiliferous lime wackestone/mudstone; locally dolomitized. Scattered branching corals locally	Dolomitized microbial laminate composed of thin microbial laminae and intervening fenestral voids. Minor detrital quartz grains. Locally silicified
Biota	<i>Operculina complanata</i> , <i>Lepidocyclus (E.) badjirraensis</i> , <i>Cycloclypeus eidae</i> , <i>Amphistegina</i> . Larger forams decrease downward into subsurface lower Mandu, which has abundant <i>Globigerina</i> and <i>Globorotalia</i> . Some small benthic forams and bryozoans present.	<i>Lepidocyclus (E.) badjirraensis</i> , <i>Operculina complanata</i> , <i>Cycloclypeus eidae</i> . <i>Lepidocyclus howchini</i> conspicuous in upper shallower water units along with some coralline algae	Scattered lepidocylinids and nummulitids present in Upper Mandu, Tulki and Lower Trealla. Articulate and encrusting coralline algae and encrusting forams, suggestive of some seagrass influence.	<i>Lepidocyclus howchini</i> , <i>Cycloclypeus</i> , coralline algae, encrusting forams, forams <i>Amphistegina</i> and <i>Marginopora</i> , minor bryozoa, echinoderms; evidence of seagrass baffles	Typically lack open marine larger forams (lepidocylinid and nummulitid) but may contain stick corals locally. Upper Trealla has <i>Astrotrillina-Flosculinella</i> assemblage (metahaline). Basal Trealla more restricted biotas (mollusk, small benthic forams), may be hypersaline.	Microbial mats

Figure 1

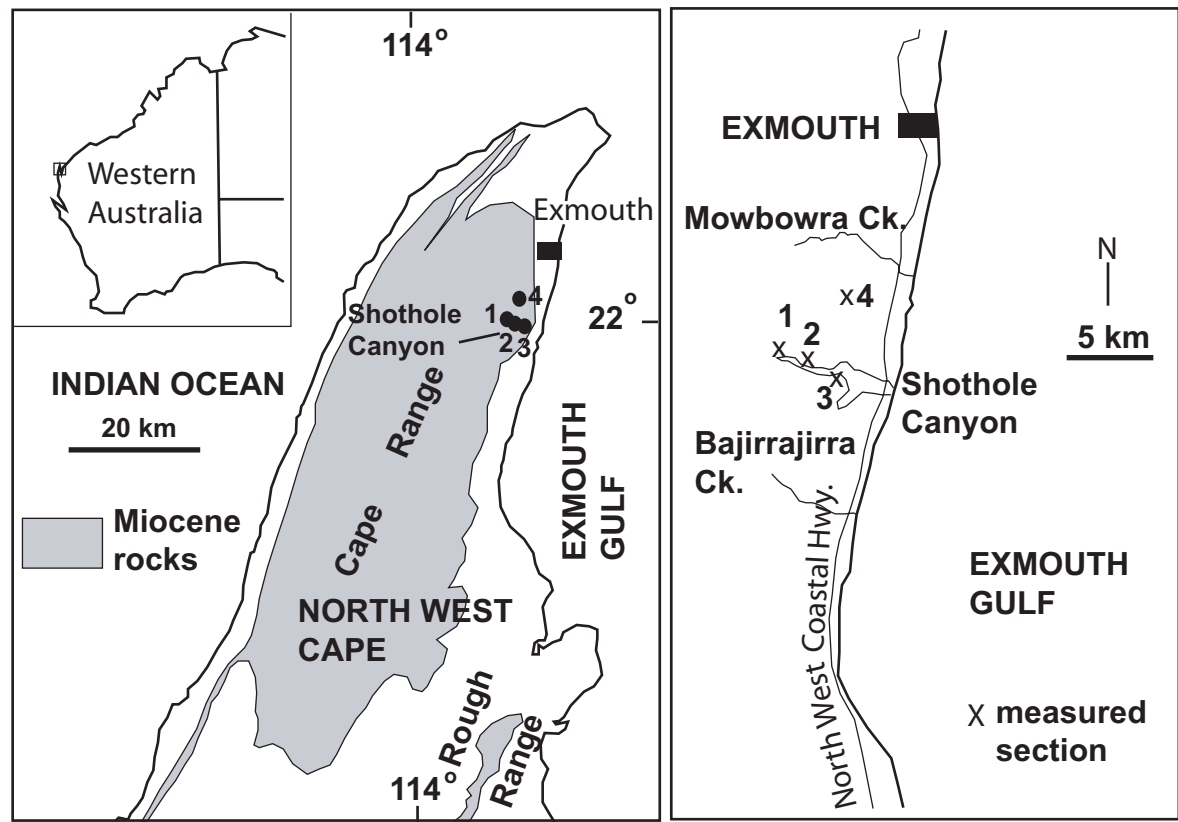


Figure 2

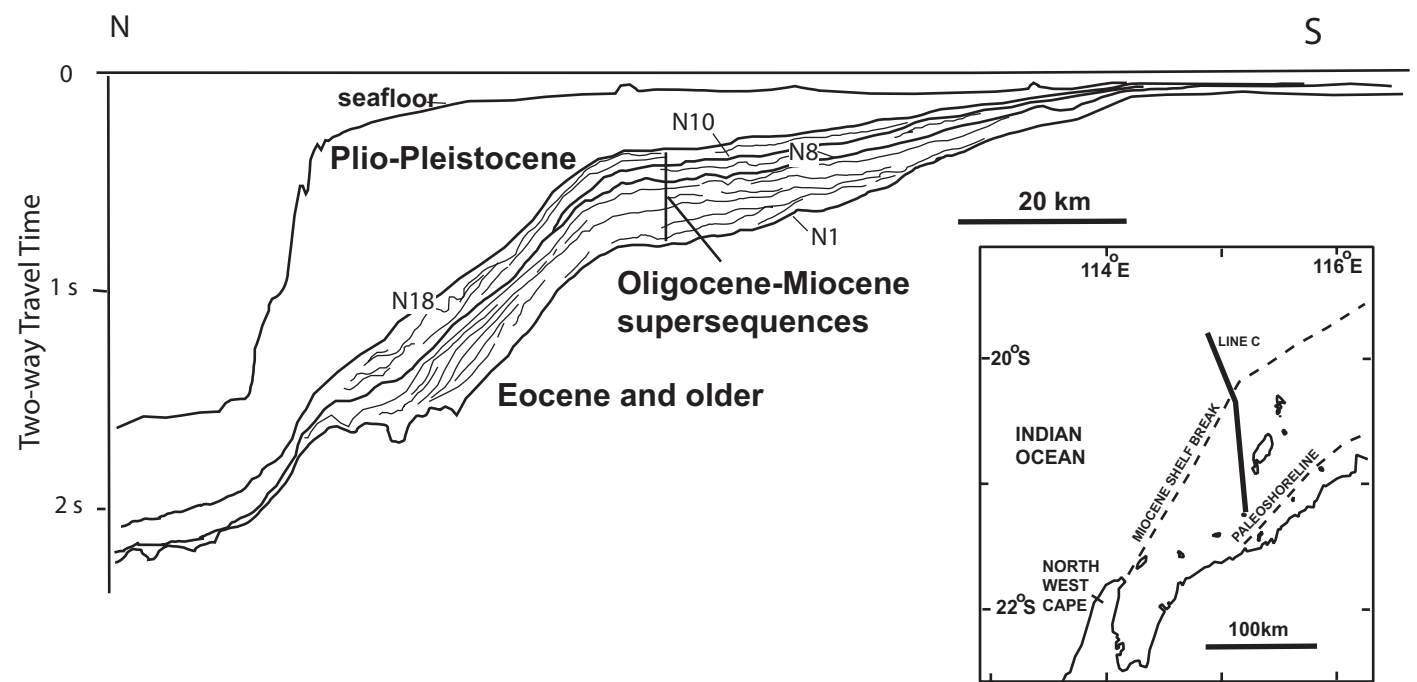


Figure 3

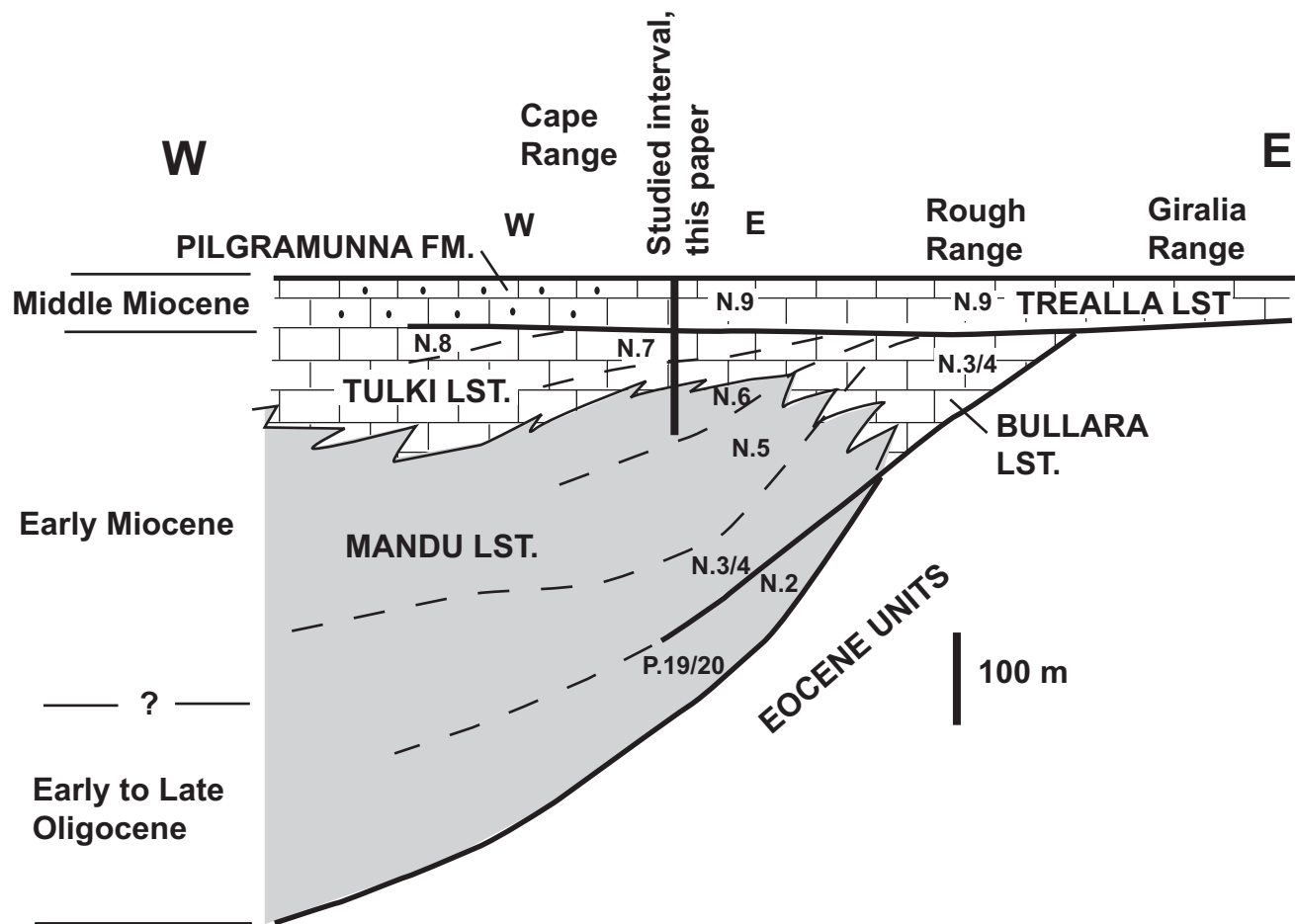


Figure 4

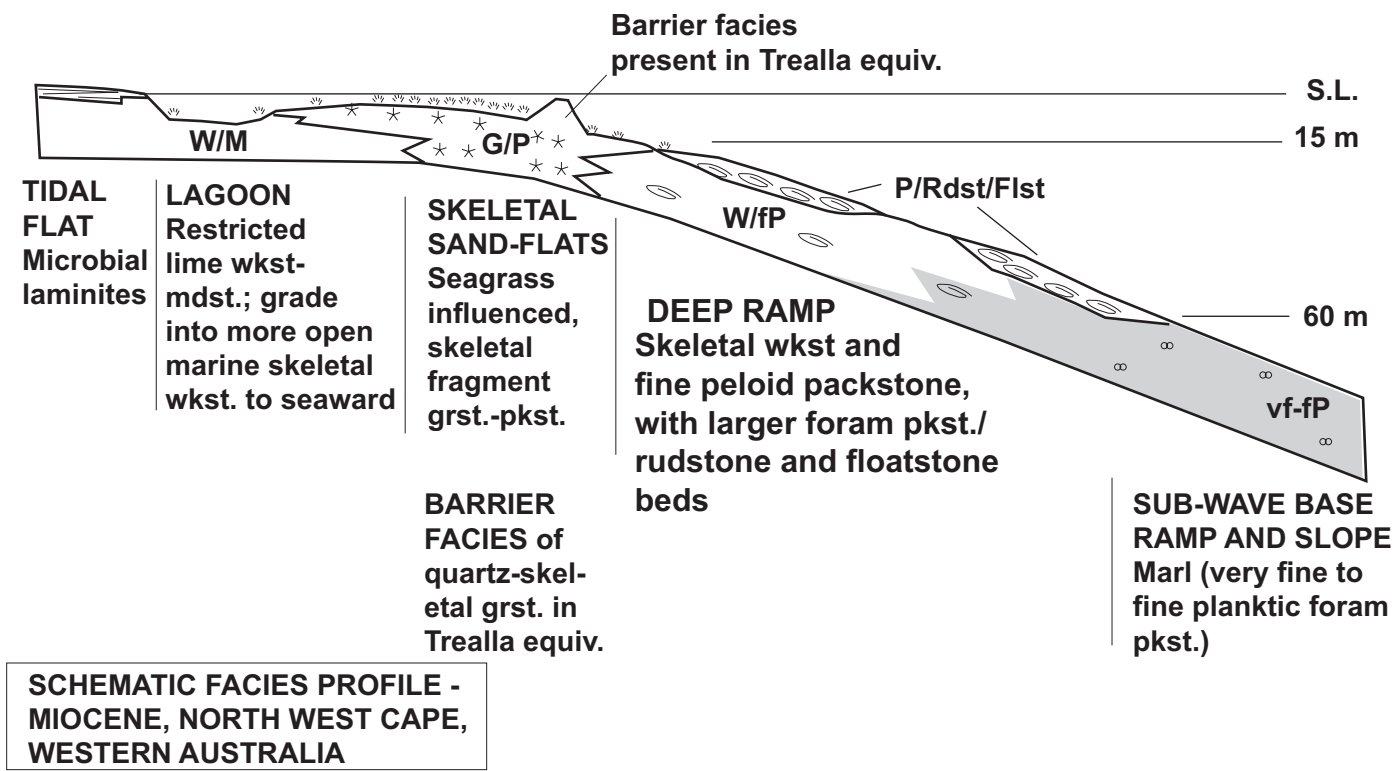


Figure 5

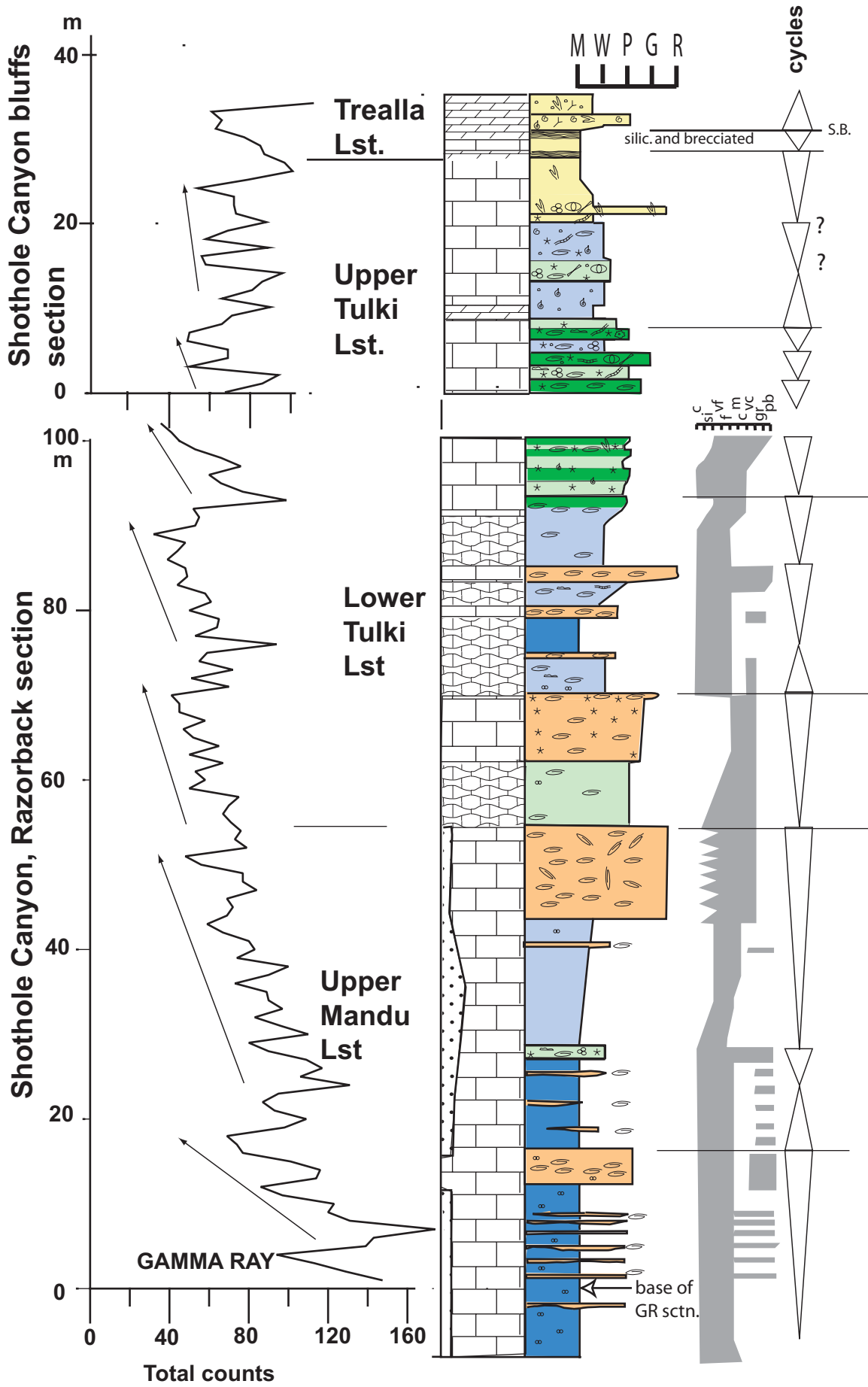


Figure 5 legend

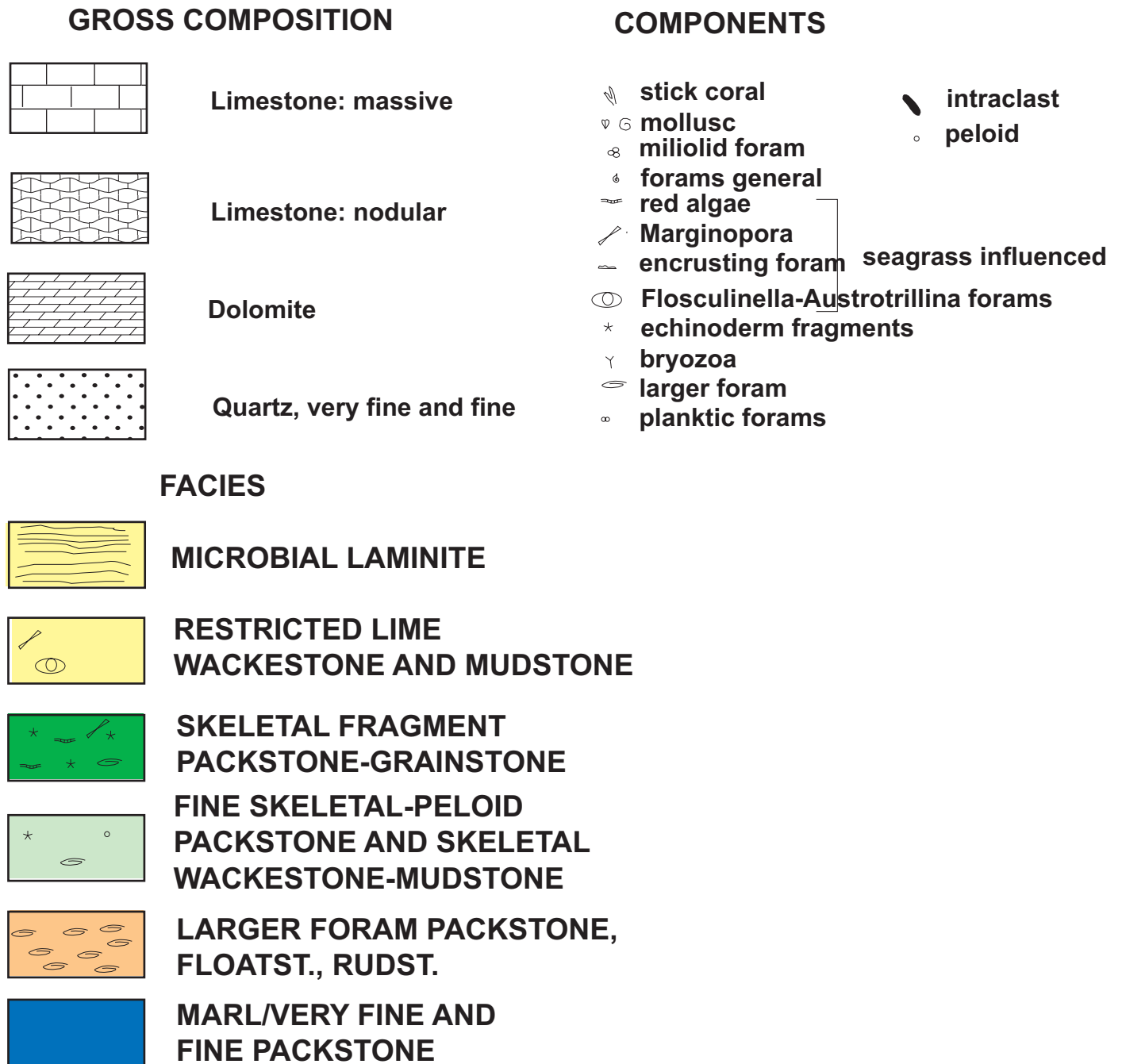


Figure 6

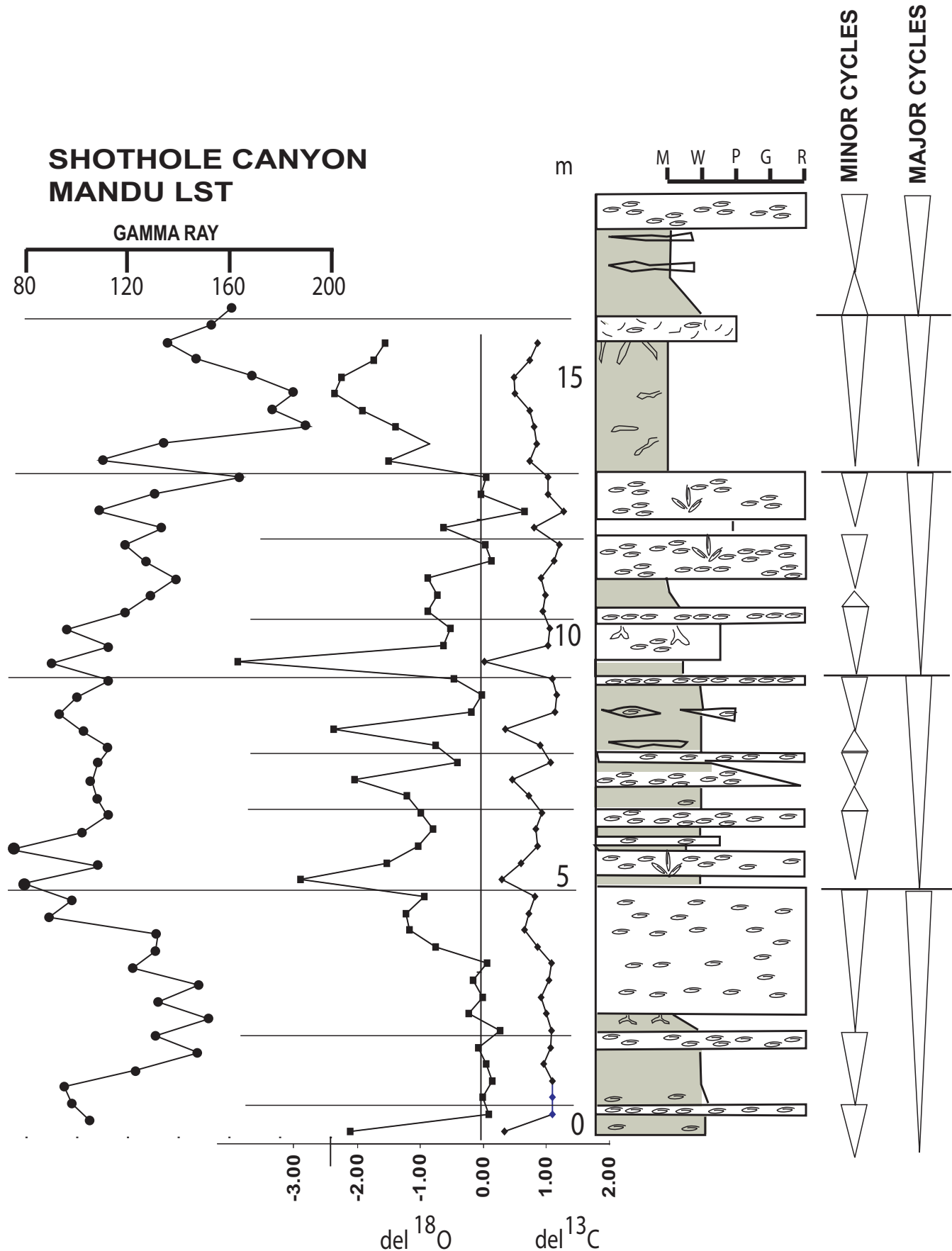


Figure 7

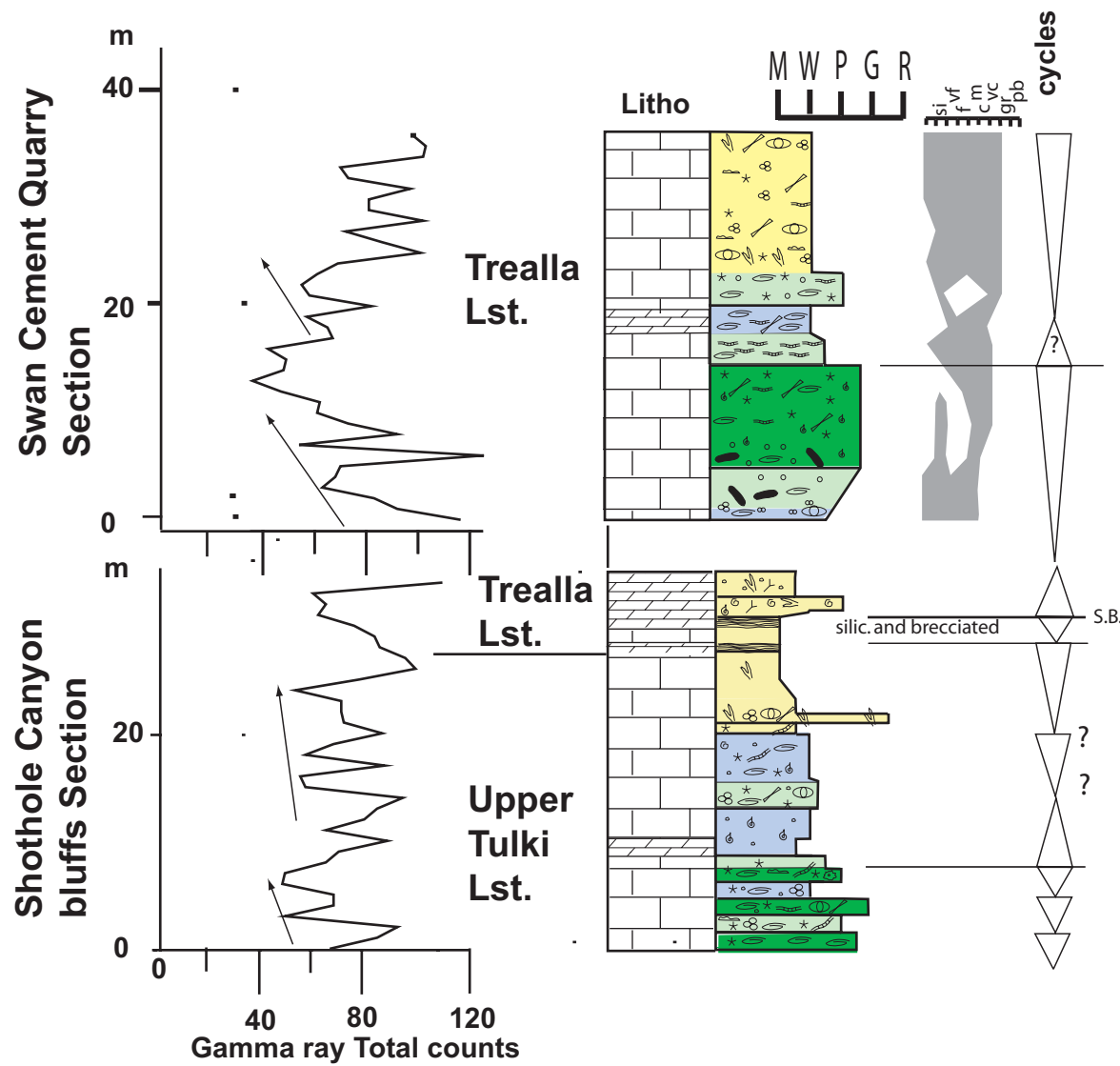


Figure 8a

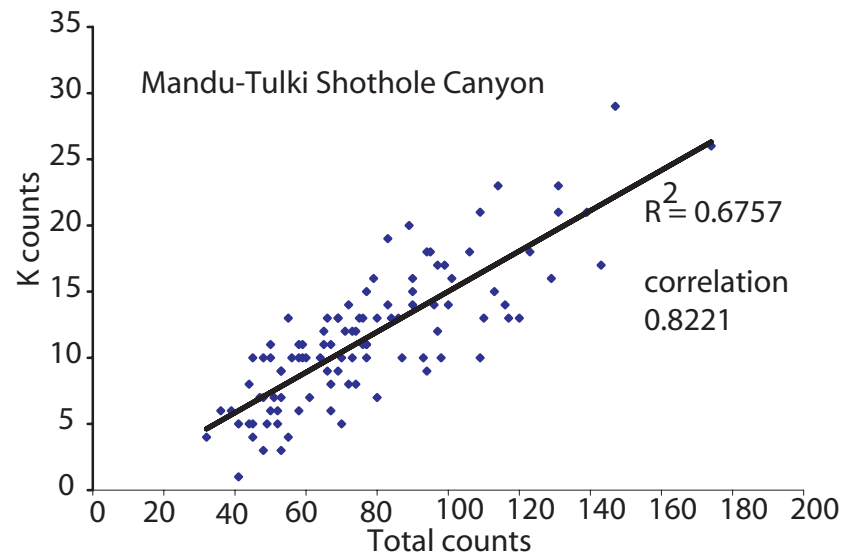


Figure 8b

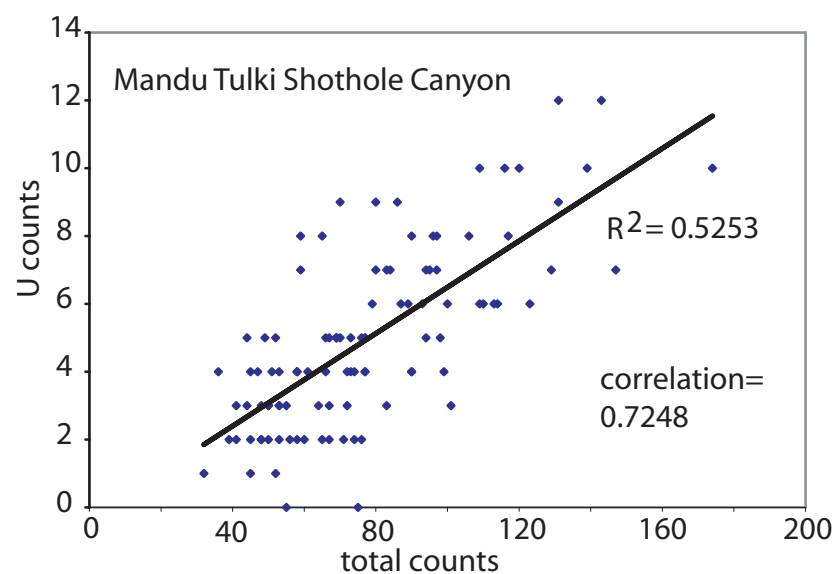


Figure 8c

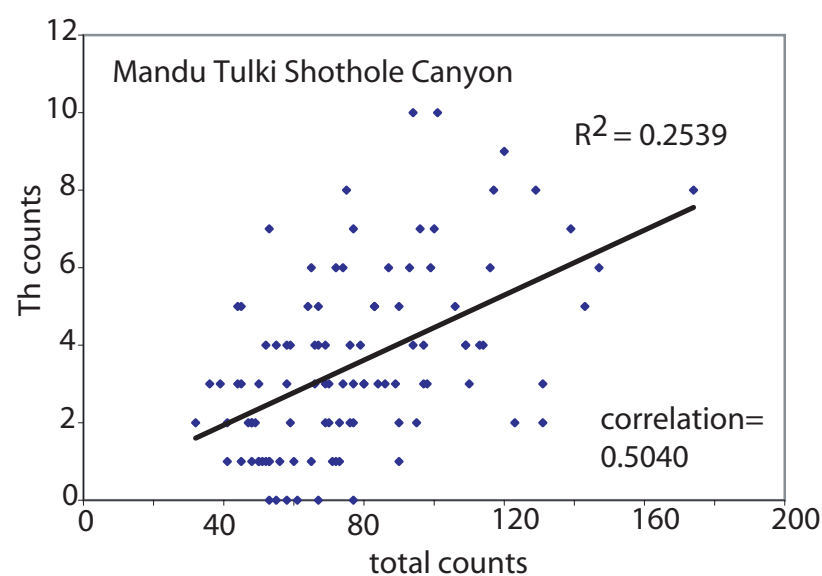


Figure 9

